

ISSN 1669-5402 (Print)

ISSN 1669-5410 (Online)



*Physiological
Mini-
Reviews*

Edited by the Argentine Physiological Society.

Vol. 1, N° 10, May 2006.

<http://www.mini.reviews.safisiol.org.ar>

Physiological Mini-Reviews

[ISSN 1669-5402 (Print); ISSN 1669-5410 (Online)]

Edited by the **Argentine Physiological Society**

Journal address: Sociedad Argentina de Fisiología, Universidad Favaloro, Solís 453 (1078),
Ciudad de Buenos Aires Argentina.
Tel.-Fax: (54) (0)11 43781151
<http://www.mini.reviews.safisiol.org.ar>

Physiological Mini-Reviews is a scientific journal, publishing brief reviews on "hot" topics in Physiology. The scope is quite broad, going from "Molecular Physiology" to "Integrated Physiological Systems". As indicated by our title it is not our intention to publish exhaustive and complete reviews. We ask to the authors concise and updated descriptions of the "state of the art" in a specific topic. Innovative and thought-provoking ideas are welcome.

Editorial Board:

Eduardo Arzt, Buenos Aires, Argentina.
Oscar Candia, New York, United States.
Daniel Cardinali, Buenos Aires, Argentina.
Hugo Carrer, Córdoba, Argentina.
Marcelino Cerejido, México City, México.
Horacio Cingolani, La Plata, Argentina.

Adolfo De Bold, Ottawa, Canada.
Osvaldo Delbono, Salem, United States.
Cecilia Hidalgo, Santiago, Chile.
Carlos Libertun, Buenos Aires, Argentina.
Gerhard Malnic, Sao Paulo, Brasil.
Raúl Marinelli, Rosario, Argentina.
Juan Saavedra, Bethesda, United States.
David Sabatini, New York, United States.

Editor in Chief: Mario Parisi.

Annual suscriptions rates are (see the electronic version for payment instructions):

- a) Printed (Institutions): 120 U\$\$ (Air mail.)
 - b) Printed (Individuals): 100 U\$\$ (Air mail. Including Safis Annual fee.)
 - c) Electronic (Individuals-.PDF): 30 U\$\$ (Including Safis Annual fee.)
 - d) Electronic (Institutions-.PDF): 50 U\$\$
-

Preparation and Submission of manuscripts:

"Physiological Mini-Reviews" will have a maximum of 2500 words, 30 references and 4 figures. Material will be addressed to scientific people in general but not restricted to specialist of the field. For citations in the text and reference list see Cerejido et al. Vol 1, N° 1. Final format will be given at the Editorial Office. Most contributions will be invited ones, but spontaneous presentations are welcome. Send your manuscript in Word format (.doc) to:
mini-reviews@safisiol.org.ar

Advertising:

For details, rates and specifications contact the Managing Editor at the Journal address e-mail:
mini-reviews@safisiol.org.ar

The "Sociedad Argentina de Fisiología" is a registered non-profit organization in Argentina.
(Resol. IGJ 763-04)

The old water channels are aquaporin proteins through which single files of water molecules cross cell membranes.

Antonio M Gutiérrez^a, Miriam Echevarría^b and Guillermo Whitembury^a

^aInstituto Venezolano de Investigaciones Científicas (IVIC), PO Box 21827, Caracas; 1020-A Venezuela

^bLaboratorio de Investigaciones Biomédicas, Departamento de Fisiología and Hospital Universitario Virgen del Rocío, Universidad de Sevilla, E-41013 Seville, Spain.
(agutierr@ivic.ve)

Running Title: *Aquaporin-Water Channels.*

We overview the critical steps leading to the demonstration that each ~28 kD protein monomer of the water channel (or pore)¹ pierce the lipid bilayer part of the cell membrane allowing the passage of ~ 10¹³ water molecules per second. The biophysical approach gives a functional and physical image of the water pore close to what has recently been obtained from the amino acid sequence, crystallography and other advances from the cloning era of trans-membrane water transport. Paracellular “wide” water channels of some leaky epithelia are not covered here [cf. Whitembury and Reuss, 1992; Whitembury and Hill, 2000].

Biophysical age.

A. Introduction.

Many of the basic hypotheses concerning the plasma membrane structure were developed in the early 1900s. Overton and Collander established that cell membrane permeability to a given substance was proportional to its lipid solubility [cf. Kleinzeller in Deamer et al. 1999, pp. 1-22]. Then evolved the lipid-sieve theory. From 1945 to date, experimental studies extended our knowledge of the role of membrane lipids and proteins that are inserted in the membrane; as in Davson and Danielli's model with trans-membrane proteins as polar pores [cf. Davson, 1989; Finkelstein, 1987].

The biophysical era produced remarkable advances concerning the water pathways; remarkable since the only signal water gives are the volume changes produced by net water movement and the signals obtained from isotopes to mark water are easily used in flat epithelia but not in small cells.

Water can cross cell membranes either by solubility-diffusion across the lipid bilayer part of the membrane, or through special channels or through both pathways. In the early 1950s, Pappenheimer, Renkin and Borrero, in Boston, and Koefoed-Johnsen and Ussing in Copenhagen, independently, found ways to differentiate between these possibilities [cf. Finkelstein, 1987; Tosteson, 1989²]. Their ideas were applied to the red blood cell (RBC) membrane by Solomon and coworkers in Boston, from 1956 on. Following a dictum

¹ The terms channel or pore will be used indistinctly.

² Tosteson, 1989, has interesting personal account-reviews by Davson (pp 15-49); Pappenheimer, (pp 363-389); Solomon, (pp 125-153); and Ussing (pp 337-362).

attributed to Galileo Galilei³, Solomon developed original stop flow methods and equipment with the millisecond time resolution needed to measure the exceedingly high water osmotic and diffusive permeabilities of RBC [cf. Solomon 1989, in Tosteson, 1989²]. Briefly, these authors realized that:

- (1) In Poiseuille's flow equation, the **water osmotic permeability**, i.e. the trans-membrane **net flow of water** secondary to application of either a hydrostatic (P_f) or an osmotic (P_{os}) trans-membrane pressure difference is proportional to the fourth power of the pathway diameter (d^4), taken as an "**equivalent cylinder**" with diameter d .
- (2) In Fick's diffusion equation, the **water diffusive permeability** (P_d), as measured with water markers (**isotope permeability**, P^*) is proportional to the second power of the pathway diameter (d^2).
- (3) Taking the permeability ratio ($(\eta_1)/(\eta_2)$, P_{os} / P_d , or P_f / P_d , or p_{os} / p_d ⁴ several unknowns cancel yielding equation 1

$$p_{os} / p_d = [2 - (1 - \alpha)^2] K d^2 + 1, \quad (\text{Eqn. 1}),$$

where the permeability ratio is proportional to d^2 , and can be solved for d ; $\alpha = \delta / d$; $K = RT/8\eta D_w V_w$; R is the gas constant; T the absolute temperature; η the water viscosity, D_w the water diffusion coefficient, δ the water molecule diameter which equals 2.8 Å, V_w the water partial molar volume, and d the pore diameter [Solomon, 1989]. A $P_{os} / P_d = 1.0$ would indicate absence of water pores. Solomon et al., found P_{os} / P_d ratios ~ 3 concluding that **equivalent** water pores were present in RBC membranes⁵.

- (4) The **temperature dependence** of P_{os} and of P_d was measured to calculate E_a , the apparent **Energy of Activation** of the RBC water permeabilities. E_a was ~ 4 kcal/mole for both permeabilities, the value for water molecules moving in free solution. This indicated a low degree of membrane-water interactions, confirming that water pores pierce the cell membrane. A high value of E_a (~ 10 kcal/mole) would indicate a high degree of membrane-water interaction suggesting that water crossed the cell membrane by solution-diffusion in the bilayer part of the membrane fabric, i.e. absence of water pores [Solomon, 1989].
- (5) Macey found that the **mercurial sulfhydryl reagent pCMBS** (para chloro-mercuri-benzene-sulphonic acid) inhibited RBC P_{os} and P_d , bringing P_{os} / P_d from ~ 3 towards 1; while E_a increased from ~ 4 to ~ 10 kcal/mole [Macey and Farmer, 1970; Solomon, 1989]. Thus, (a) the **RBC water pores were proteins**; (b) **pCMBS** "closed" them; and (c) the ~ 10 % water permeabilities remaining with **pCMBS** reflected, water movement through the lipid bilayer part of the membrane.

³ "When experimenting, measure what can be measured and make measurable which as yet cannot be measured".

⁴ In Eqn 1 permeabilities per channel (p), rather than trans-membrane permeabilities (P) are used, since $P = p \times n$. Where n , the number of channels per unit membrane area; and n cancels when the permeability ratios are taken [cf. [fig 1](#)]

⁵ These concepts from macroscopic hydrodynamic theories surprisingly hold down to "pores" with d only slightly larger than the water molecule δ [cf. Solomon, 1989, Finkelstein, 1987].

- (6) The limited interaction between water and urea, as both crossed the RBC membranes, indicated urea (molecular diameter $\sim 5.4 \text{ \AA}$) did not move freely through the water pore [Macey and Farmer, 1970; Finkelstein, 1987, 1993; Parisi, 1983]; therefore, since d had to be smaller than 5.4 \AA , there was not enough room for two water molecules (with a width $2\delta = 2 \times 2.8$ or 5.6 \AA) to fit side by side; i.e. there was space for only one line of water molecules to move in single file through the water pore.

It has been shown that for single file pores, P_{os} / P_d gives the number of water molecules single-filing within the channel rather than the pore diameter (**fig. 1**) [Finkelstein, 1987, 1993]. Therefore, it is important to explain here why when d diminishes below 5.6 \AA , p_{os}/p_d does not lead to the pore diameter value, but rather to considerations related to a single file water channel. This may be done with the aid of the blue line in **fig. 1**, which is the theoretical fit of p_{os}/p_d or p_{os}/p^* as a function of d . \circ is p_{os} / p_d for amphotericin B (Ampho B in **fig. 1**, with $d = 8 \text{ \AA}$) and nystatin channels [cf. Finkelstein, 1987]. The permeability ratios for nystatin and amphotericin B fall on the theoretical line. Therefore, for pores of this d , p_d values (obtained with markers) truly represent the diffusive permeability coefficient within the pore (p_d) and d is obtained from p_{os} / p_d by means of equation 1, as was used to obtain the blue theoretical curves of this **fig**. When the pore diameter falls below $d = 5.6 \text{ \AA}$ (twice δ), water molecules cannot overtake each other within the pore. Then, p^* underestimates p_d , because the specific activity of the water isotope within the pore does not represent the specific activity of the free solution. Therefore, at $d < 5.6 \text{ \AA}$, $(p_{os} / p_d) < (p_{os} / p^*)$. In other words, if one were to calculate d from (p_{os} / p^*) , one would obtain the falsely large figure for d of $\sim 12 \text{ \AA}$. This is illustrated as \blacktriangledown in **fig. 1**. \blacktriangledown represents p_{os} / p^* for the well studied gramicidin A pore (Grami A in **fig 1**). Inside Grami A, with a well known, $d = 4 \text{ \AA}$, water permeation is known to be single-file [Finkelstein, 1987, 1993], \blacktriangledown is well above the theoretical prediction. As the dashed line emphasizes, p_{os} / p^* overestimates p_{os} / p_d , because p^* is an underestimate of p_d [cf. Finkelstein, 1987, 1993].

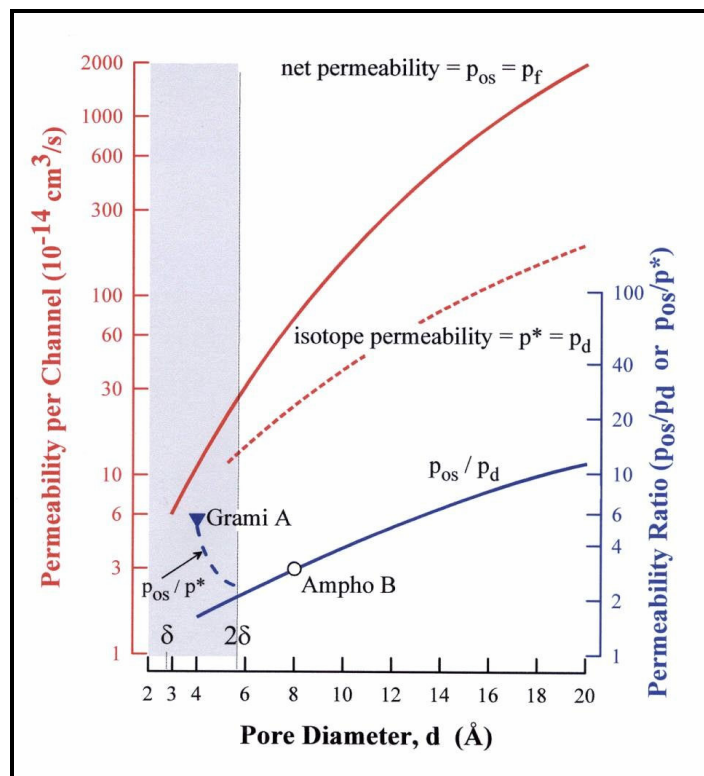


Figure 1. Permeabilities per channel (p) (l.h.side ordinate, red) vs pore diameter (d). The red continuous line is single pore p_{os} (or p_f) vs d in the range of 2.8 to 20 Å for a straight cylinder. The red dashed line is single pore diffusive permeability (p_d) equal to the isotope permeability (p^*). It stops at $d = 5.6$ Å (vertical line). The right hand blue ordinate is p_{os}/p_d or p_{os}/p^* , which is plotted vs d as the blue continuous line. The shaded area indicates that at $d < 5.6$ Å, p_{os}/p_d and p_{os}/p^* differ. \circ is p_{os}/p_d for amphotericin B (Ampho B) and nystatin channels ($d = 8$ Å), whose permeability ratio falls on the theoretical line. ∇ is p_{os}/p_d for the gramicidin A (Grami A) channel, through which water single-files [Finkelstein, 1987]. The difference between the blue dashed line joining ∇ and the blue continuous line illustrates that $p_{os}/p^* > p_{os}/p_d$, because p^* is an underestimate of p_d . Eqn 1 was used in the calculations [modified from Whittembury and Reuss, 1992].

B. Peritubular cell membrane Osmotic Permeability, P_{os}^{cb} , of the rabbit kidney PST: control experiments; effects of pCMBS; effect of Temperature; values of E_a .

We extended these observations to epithelial cells, since only RBC had been used in the above observations. We used rabbit kidney proximal straight tubule (PST). Methods precise enough to measure P_{os} and P_d in PST were developed with 50-60 ms time, and 30 nm space resolution. One PST dissected out of rabbit kidneys was held, in a chamber with micro pipettes. The outside bath was changed (within 80 ms) to a 30 mOsm/l anisotonic solution. The ensuing cell and lumen diameter (i.e. volume) changes were recorded **on line** with an original image processor [Whittembury et al., 1986]. In the control experiments P_{os}^{cb} was found to be $\sim 50-90 \times 10^{-4} \text{ cm}^3/\text{s}$. per cm^2 of basal membrane area per Osmolar transmembrane osmotic pressure difference, which decreased to ~ 15 to 20 % of this value with pCMBS. E_a (kcal/mol) was ~ 3.2 (controls) and ~ 9.2 (pCMBS-treated tubules). Therefore, proteinic aqueous pores pierce PST basolateral cell membranes which are reversibly "closed" by pCMBS ⁶, since these actions of pCMBS (and Mersalyl) reverted with 5 mM Dithiothreitol (DTT) [cf. Whittembury et al., 1984]

C. PST cell membrane diffusive permeability, P_d . Ratios of P_{os}/P_d .

To calculate P_d , proton nuclear magnetic resonance of suspended cells and diffusion coefficient of $^3\text{H}_2\text{O}$ in packed isolated PST cells were measured. Both methods coincided: 197 and 193 $\mu\text{m}^2/\text{s}$ in the controls, respectively. This value decreased to 14 $\mu\text{m}^2/\text{s}$ with pCMBS and was reverted with DTT. E_a was ~ 2.9 (controls) and 9.0 (pCMBS). The calculated control P_{os}/P_d ratio was ~ 15 , and was reduced to ~ 2.5 with pCMBS, indicating that this mercurial "closes" the water pores [Echevarría et al., 1994, Whittembury and Reuss, 1992]. A pore diameter d calculated from a P_{os}/P_d ratio of 15 would be ~ 24 Å, an unreal value incompatible with the fact that PST cell membranes are known to exclude solutes like raffinose, sucrose and mannitol, with molecular diameters by far smaller than 24 Å. As reasoned above, the PST water pore could be a single file channel. This could be firmly concluded from the sieving properties of the water pore; therefore, we studied interaction between water and solutes.

⁶ Mersalyl also decreased P_{os}^{cb} *in vitro* and *in vivo*, at therapeutic doses. It is possible that part of the action of the "old mercurial diuretics" could be due to their action on P_{os}^{cb} [Whittembury et al., 1984].

D. Water Solute Interactions: Graded size non-electrolytes reflection coefficients (σ) indicated water moves in single file through the Water Pore.

With the method outlined in B, tubules were challenged for 20 s. with an bath made 35 mOsm/kg hyper-osmolar by addition of either **NaCl**, **KCl**, raffinose (**R**), sucrose (**S**), mannitol (**M**), glycerol (**G**), ethyleneglycol (**E**), urea (**U**), acetamide (**A**) or formamide (**F**). With all solutes (except **F**) tubules shrunk osmotically within 500 ms of the osmotic challenge and remained shrunk, without recovering their original volume. The reflection coefficients σ equaled 1.00 for all molecules (except for **F**). With **F**, tubules barely shrunk and quickly recovered their original volume. Thus $\sigma \ll 1.00$ (~ 0.62) for **F**. As mentioned in section A (§6) these results indicated that within the water pore water must move in a single file, because **G**, **E**, **U** and **A** do not permeate the pore. Therefore, also for the PST membrane water pore, **d** would be too narrow for water molecules ($\delta = 2.8 \text{ \AA}$) to be able to overtake each other within it [cf. Parisi and Bourguet, 1983].

In retrospect in the case of **F**, with $\sigma \sim 0.62$, we used correction factors that misled us to conclude that **F** also permeated the water pore, and we wrongly assigned a **d** value of 4.2-4.7 \AA for the water channel [Gutiérrez et al., 1995]. Recent studies of Aquaporin-1 indicate that **d** in the narrow part of the selectivity filter is only slightly wider than the water molecule diameter δ of 2.8 \AA [Agre, 2004].

E. Length of the Selectivity Filter of the Water Pore.

Solution to this problem was approximated in two forms: (a) Using single file equations where P_{os} / P_d ratios lead to **N** the number of water molecules in line within the narrow part of the pore (the pore selectivity filter) [cf. Finkelstein, 1987]. A first approximation leads to $N = 15-18$ from our P_{os} / P_d ratios. (b) Bimodal theory equations indicate the selectivity filter would hold 4 - 6 water molecules over a length of perhaps 16-20 \AA [Whittembury et al., 1997]. These theoretical predictions agree with recent electron diffraction and model building [Agre, 2004]. (c) Clearly a wider region must link the single file selectivity filter with the outside and inside solutions bathing the membrane [Whittembury et al., 1997]. This picture is remarkably close to the "Hour glass " model [Jung et al., 1994, Ref. 12 in Agre, 2004].

The age of cloning and molecular biology.

A. Aquaporins revolution came by serendipity

After many years of biophysical evidences for the presence of specific proteins responsible for water movement across cell membranes, which are reviewed above, the molecular identification of the first water channel came in 1992 with the discovery of CHIP28 [Preston et al, 1992-Ref. 7, in Agre 2004], a protein known today as Aquaporin-1 (AQP1). Peter Agre and his group, studying membrane proteins related to the Rh group in red blood cells, isolated a smaller protein (28kDa) that always co purified with the 32 kDa Rh-protein of their interest. The amino acids identification of some regions of this protein was followed by the cDNA cloning of the gene from a human bone marrow library. Therefore, they had good knowledge of this protein --including their multisubunit structure (Smith, 1991, Ref 5, in Agre, 2004), when in vitro transcription and injection of its cRNA on

Xenopus oocytes led them to discover, after hypoosmotic challenging of the oocyte, that CHIP28 was indeed a cell membrane water channel [Agre, 2004]. Aquaporins are members of the major intrinsic protein (MIP) superfamily of integral membrane proteins that function as specialized water channels to facilitate transport of water in cell membranes of animals, plants, bacteria and fungi.

Today, thirteen aquaporins have been identified in man. From their genome structure they can be divided into four groups: i) AQP0, 1, 2, 4, 5, 6; ii) AQP3, 7, 9, 10; iii) AQP8; and iv) AQP11, 12. From their selectivity they are grouped into (a) strictly water-selective (AQP0, 1, 2, 4, 5, 8), or (b) also permeable to glycerol (AQP3, 7, 9, 10) called aquaglyceroporins.

B. Structure of aquaporins.

AQPs are small proteins with molecular weights that vary from 26 to 35 kDa. The primary sequence (**Fig. 2a**) forms two tandem repeats of three membrane-spanning α -helices domains (1-6), connected by loops (A-E), with the amino and carboxy termini oriented toward the cytoplasm. Loops B (cytoplasmic) and E (extracellular) contain an Asp-Pro-Ala (NPA) motif that is connected to each other by the folding back inside the membrane of both loops, forming a single transmembrane water pore through each aquaporin subunit (**Fig. 2b**). The resulting structure, of a central narrow constriction that opens wider toward both sides of the membrane is known as the hourglass model. In the membrane, AQPs form tetramers in which each subunit contains a water channel (**Fig. 2c**). A tetrameric arrangement confers to the monomer a most stable conformation inside the membrane. The three-dimensional structure of AQP1, determined by cryo-electron microscopy of two-dimensional crystals of the protein [Walz et al, 1997], confirmed the basic structural organization proposed for each subunit of AQP1 and the formation of the tetrameric complex in the membrane.

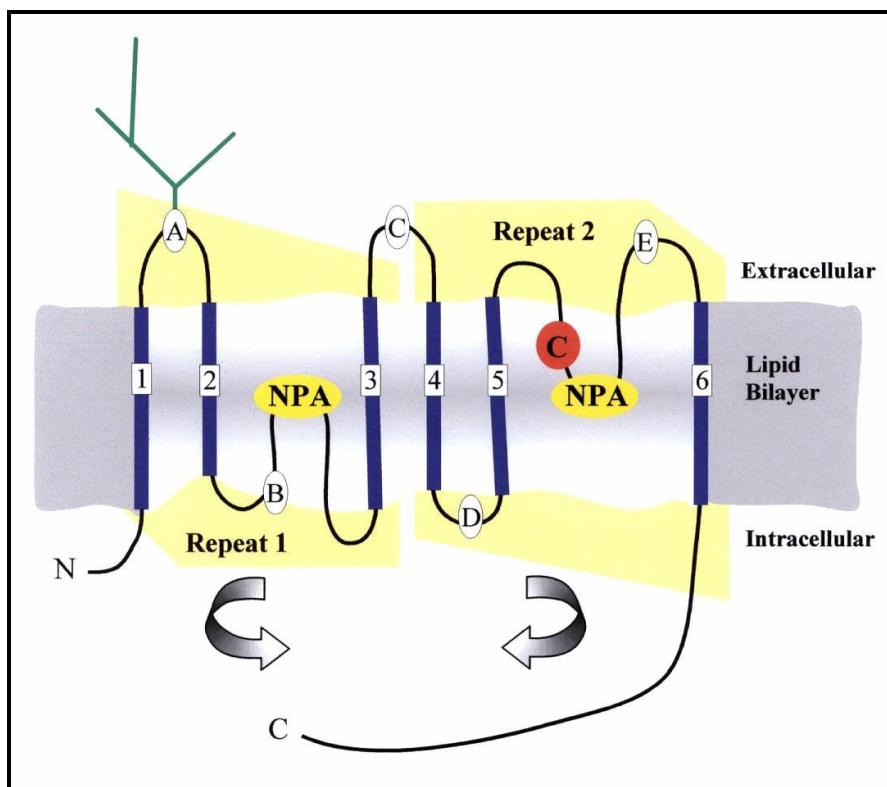


Figure 2a. Membrane orientation of one AQP1 subunit predicted from primary amino acid sequence (Schema). Two tandem repeat units of the protein; each with three bilayer-spanning domains (1, 2, 3, for repeat 1; and 4, 5, 6, for repeat 2) are oriented 180° with respect to each other. They are joined by five loops (A to E). Loops B and E contain the conserved motif Asparagine, Proline, Alanine [Asn-Pro-Ala, NPA]. Cysteine 189 (C), controls pore permeability when blocked by pCMBS and HgCl₂ [cf. Agre, 2004, Ref. 11]. Loop A has a glycosylation site (green).

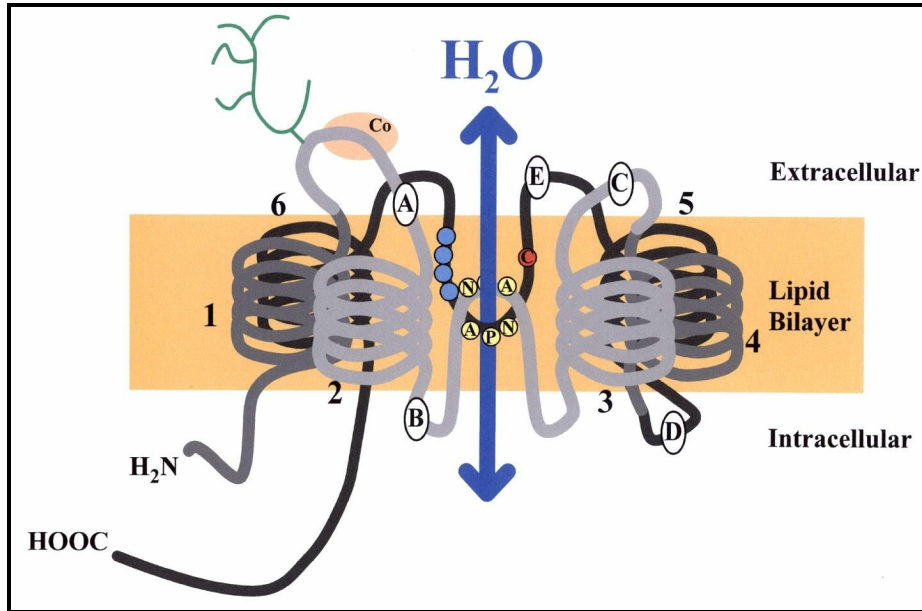


Figure 2b. Hourglass model for the membrane topology of one AQP1 subunit (Schema). Co The region related to Rh blood group system, Colton antigens is Co [Smith et al., 1994, Ref. 23 in Agre, 2004]. Blue circles are highly conserved amino acids among AQPs. C is cysteine 189. Folding of loops B and E overlap within the lipid bilayer to form a single aqueous pore.

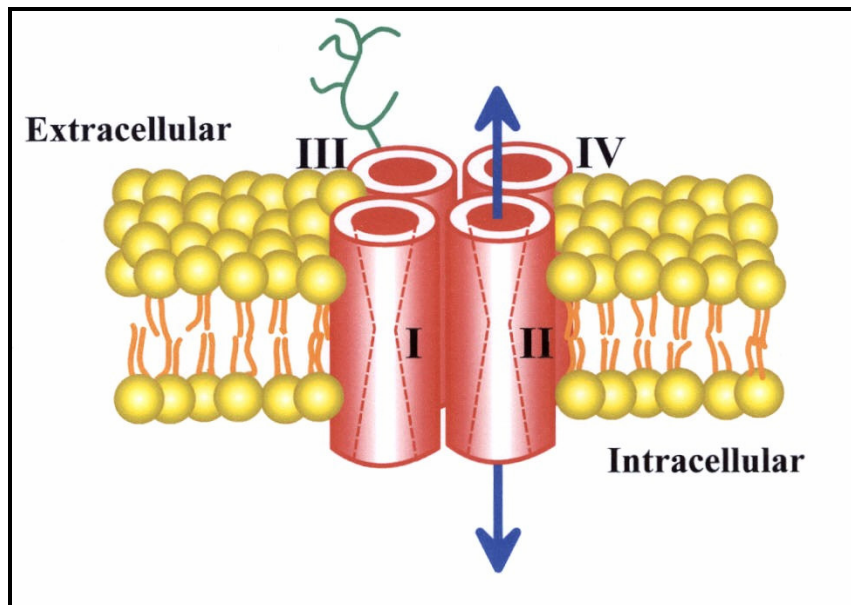


Figure 2c. Four AQP1 subunits (I, II, III, IV), each being a water pore, keep together as a tetramer.

Finally, the atomic structure of AQP1 was determined at 3.8 Å resolution (Murata et al, 2000, ref. 14 in Agre, 2004) and enabled a precise correlation between specific amino acids and three-dimensional structure of the protein. Crystallographic images confirmed that the six α -helices transmembrane domains form a right-handed bundle in which the stability is maintained due to the large crossing angles of the helices, local fits between helix ridges and grooves, and interactions between highly conserved glycines at the crossing sites. Also, confirmed that loops B and E, are short α -helices that project to the center of the bundle in a 90° angle to form the narrow water pathway of the channel (**Fig.3**). Both loops interact by the two NPA triplets and are held together by van der Waals forces established between prolines (Pro). The two asparagines (Asp) converge to partially delimit the narrowest path of the channel (~3 Å). The hydrophobic surface lining the inside of the pore adjacent to the two Asp (76 of loop B, and 192 of loop E) of the NPA motifs, is formed by Ile 60 (helix 2), Phe 24 (helix 1), Leu149 (helix4) and Val 176 (helix 5).

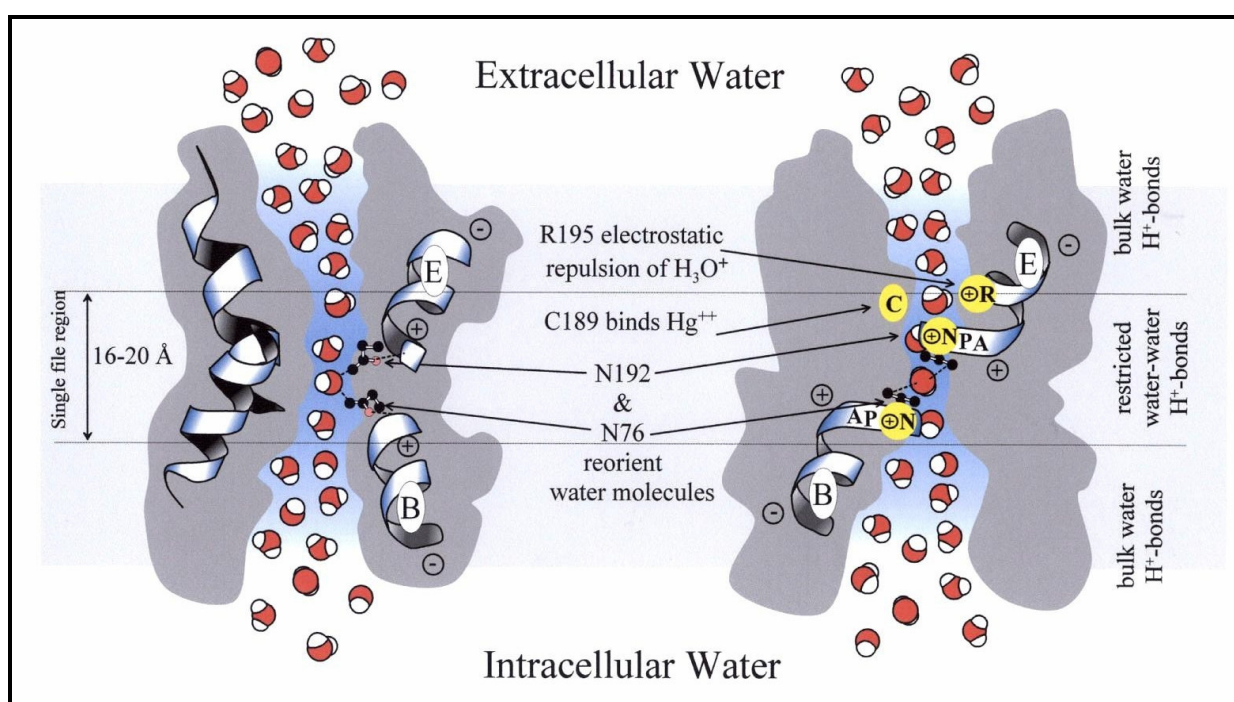


Figure 3. Schema of a sagittal cross section of one AQP1 subunit illustrating how water molecules flow through. The wide extra- and intra-cellular parts of the pore are separated by a ~16-20 Å long narrow region through which water dipoles single file [Whittembury et al., 1997]. In the wide regions water dipoles keep among themselves their usual H-bonds (not shown). In the single file region water dipoles interact with pore-lining residues that prevent H-bond formation between water molecules. Electrostatic repulsion is believed to be created by a fixed positive charge from the pore-lining arginine (R195). Note that water dipoles reorient themselves because their oxygens H-bond with the asparagines N192 and N76 from the NPA triplets. Other amino acids contribute to physical restriction. All this prevents Grotthus-type proton translocation along a chain. Modified from Agre, 2004.

C. Molecular bases for AQP1's selectivity.

In general, AQPs are impermeable to charged solutes and ions, including protons. Physical narrowness of the aqueous pore is not the only explanation for the selectivity of these proteins. According to the atomic model of AQP1, the selectivity of the pore constriction is critically determined by the two Asn residues (Asn 76 and Asn 192)

protruding with their amido groups toward the lumen of the pore, and by the positive electrostatic field generated toward the center of the pore by the orientation of helix B and E with its C-termini facing out of the pore. Hence, when a water molecule comes close to the membrane center the oxygen atom orients itself to form hydrogen bonds with those amido groups, breaking for that the Hydrogen bonds to its neighbor water molecules and instead establishing H-bonds, first one, and then two, with the Asp residues (**Fig 3**). In the pore constriction, the water molecule can form hydrogen bonds only via the oxygen but neither through its hydrogen atoms, nor to the hydrophobic walls of the pore. As a consequence, water molecules can permeate the pore, but breaking the continuity of the string of hydrogen bonds abolishes transfer of protons that would occur in bulk water [Murata, et al, 2000, ref. 14 in Agre, 2004, Tajkhorshid et al, 2002, Ref. 18 in Agre, 2004].

AQP1 had been also reported be permeable to CO₂. Cells expressing AQP1 [Cooper et al, 2002] show a rate of pHi-lowering, after bubbling the extracellular solution with CO₂, that is significantly faster than in conditions of lack of CO₂ or mercurial blocking of the protein. These experiments indicate that CO₂ transport across the plasma membrane is facilitated by AQP1, although more physiological approximations are desirable to clarify contradictory data and even to broaden the possible role of AQP1 as a channel permeable to other volatile molecules.

D. Tissue distribution and regulation of Aquaporins.

Aquaporins are widely distributed, and with few exceptions, they are present in practically all cell types in the human body [Takata et al., 2004]. Table 1, summarizes the tissue distribution for each AQP. In organs typically involved in large transit of water as the kidney, often more than one AQP is present. Distribution of each AQP is very particular, some are ubiquitous (AQP1, 3, 8 and 9), while others are expressed in unique tissues (AQP0 and AQP2). Three AQPs are present in brain (AQP1, 4 and 9) [Amiry-Moghaddam and Ottersen, 2003, Ref. 45 in Agre, 2004]. AQP1 is expressed in apical membrane of choroid plexus epithelial cells, while AQP4 expressed in basolateral membrane of ependymal cells, end-feet domains of astrocytes surrounding brain capillaries and on glial lamella of osmosensitive regions. Brain distribution of AQP9 is less known but recently its expression on neurons have been described.

AQPs are integral proteins of the cell membrane, except for AQP6, 11 and 12 that are permanently located in intracellular vesicles. Water permeability through AQPs is variable. Some are highly permeable as AQP1 (3×10^9 water molecules/sec, per monomer), and in others, water permeability is low (as AQP0), or regulated by hormones and/or extracellular factors as pH. Some AQPs have conserved phosphorylation sequences for protein kinase A (AQP2, 5 and 9) or protein kinase C (AQP4, 5 and 7) that probably regulate the gating or subcellular distribution of these proteins. For instances, vasopressin-induced water permeability strictly depend on the direct Ser-256 phosphorylation of AQP2. By other hand, protons concentration gated the water and glycerol permeability of AQP3 [Zeuthen and Klerke, 1999, Ref. 61 in Agre, 2004] and, AQP6 becomes permeable to water and chloride by conformational changes occurring at pH < 5.5 [Yasui et al, 1999]. AQPs, like AQP1, 2, 5, and 8, can exhibit a dual location, and under action of specific hormones translocate between intracellular AQP-bearing vesicles and the apical cell membrane. AQP2, in the principal cells of renal collecting ducts, remains after synthesis in cytosolic-vesicles. The vasopressin-induced rise of cAMP, via V2 receptors, triggers a complex mechanism that guides the fusion of AQP2-bearing

vesicles to the apical plasma membrane, thus rendering the membrane permeable to water [Nielsen et al, 1993, Ref 21 in Agre, 2004; Ford et al., 2005].

Mercurial reagents, like HgCl₂ or pCMBS inhibit the water permeability of most known AQPs [Whittembury et al, 1984, Echevarría et al, 1993] by interaction with a cysteine residue located close to either the first or second NPA repeat of the aqueous pore (**Fig. 2a**). However, AQP4 permeability is not affected by mercurials and exposure to HgCl₂ of AQP6 significantly increase its water permeability. Transcriptional regulation of AQPs expression has also been described. In kidney, water deprivation increased the mRNAs for AQP2, 3 and 4 [Murillo et al, 1999]. Chronic rise of vasopressin upregulates the AQP2 mRNA expression due to direct interaction of cAMP with specific responsive elements on its promoter. In lung, treatments with corticoids induce expression of AQP1.

E. AQPs and pathologies.

Today many pathologies are associated with alterations in some AQP. A large variety of conditions in which water handling is abnormal are associated with renal dysfunction, and in many of them participation of AQPs is being demonstrated. Among the different forms of inherited nephrogenic diabetes insipidus (NDI), one is associated with mutations on AQP2 that make the protein either non-functional or unable to travel to the membrane (de Mattia et al, 2005). Therefore responsiveness to vasopressin is critically impeded in these patients and abundant polyuria is observed. Moreover, conditions in which acquired NDI is observed, as in lithium treatment in psychiatric patients, bilateral urethral obstruction, chronic hypercalcemia or hypokalemia, compulsive water drinking, chronic renal failure, or age-induced-NDI, a reduced expression of AQP2 in collecting duct cells of animal models is always observed. On the contrary increase expression of AQP2 is observed on the syndrome of inappropriate secretion of antidiuretic hormone (SIADH), congestive heart failure, and during pregnancy (Nielsen et al, 2002). In the eye, fluid transport is important and requires expression of several AQPs. In processes such as maintenance of intraocular pressure (AQP1 and 4), corneal and lens transparency (AQP0, 1, and 5), visual signal transduction (AQP4), tear formation and conjunctival barrier function (AQP3 and 5), the appropriate expression and functioning of these proteins is needed. For instances, mutations in AQP0 are associated with cataracts formation. An important role on glycerol metabolism for AQP3 and AQP7 had been reported. A remarkable fat mass accumulation and larger adipocytes size was observed in AQP7 null mice when compared to wild type mice. These experiments provide basis to investigate whether upregulation of AQP7 might be utilized as a therapy for some forms of obesity. Brain edema is a major cause of mortality in pathologies as stroke, brain tumour, trauma, viral infections, and some diseases that show brain-inflammation, as liver failure. Studies in AQP4-knockout mice (Verkman, 2005) provide strong evidences for the involvement of AQP4 in either the entry or the exit of water into and from the brain. Therefore, regulation of AQP4 function or expression may be targets to control brain edema. Additionally, AQP4 in end-feet membrane of astrocytes have been demonstrated to participate on K⁺ clearance from synaptic space after neuronal activity. Animals models with altered astrocytes AQP4 distribution showed an increase of epileptic seizure severity that strongly suggest a role for this protein on pathological conditions associated with altered brain ion homeostasis.

Table 1. Tissue distribution of AQPs.

Aquaporin	Distribution
AQP0	Eye (crystalline)
AQP1	Erythrocytes, Brain, Kidney, Trachea, Heart, Placenta, Uterus, Urinary Bladder and Urethra, Gall-bladder, Testis, Lung, Bronchus, Bile Duct, Skin, Vascular endothelium, Eye
AQP2	Kidney (Collecting duct)
AQP3	Kidney, Gastrointestinal tract, Liver, Pancreas, Spleen, Prostate, Eye, Sweat and Lachrymal glands, Lung, Erythrocytes, Uterus, Urinary Bladder and Urethra
AQP4	Brain, Gastrointestinal tract, Kidney, Bone marrow, Lung, Skeletal muscle, Eye, Lachrymal gland, Ear
AQP5	Salivary gland, Lachrymal gland, Lung, Gastrointestinal tract, Eye
AQP6	Kidney
AQP7	Spermatozoids, Testis, Adipose tissue, Kidney, Heart, Skeletal muscle, Gastrointestinal tract
AQP8	Liver, Pancreas, Testis, Placenta, Uterus, Salivary gland, Small intestine, Colon, Gall-bladder, Heart
AQP9	Adipose tissue, Heart, Colon, Leucocytes, Liver, Brain, Kidney, Small intestine, Lung, Spleen, Testis, Bone marrow
AQP10	Small intestine
AQP11	Kidney
AQP12	Pancreas, Eye

Acknowledgements

It is a pleasure to thank Mr. LF Alvarez and Mr. Mardonio Díaz for their help. This work was supported by grants from Instituto de Salud Carlos III PI 030296 and Junta de Andalucía, 68/04 to M E. and from the Venezuelan Research Council (CONICIT, FONACIT) and Fundación Polar to GW. and AMG.

REFERENCES

1. **Agre, P.** Aquaporin Water Channels (Noble Lecture). *Angew. Chem. Int. Ed.* 2004; 43: 4278-4290.
2. **Amiry-Moghaddam M, Ottersen OP.** The molecular basis of water transport in the brain. *Nature Reviews* 2003; 4: 991-1001.
3. **Cooper GJ, Zhou Y, Bouyer P, Grichtchenko II, Boron WF.** Transport of volatile solutes through AQP1. *J. Physiol* 2002; 542: 17-29.
4. **Deamer DW, Kleinzeller A, Fambrough DM.** Membrane Permeability, 100 years since Ernest Overton. *Current topics in Membranes.* Academic Press, N York. 1999; 48: 423pp.
5. **De Mattia F, Savelkoul PJ, Kamstee EJ, Konings IB, van der Sluijs P, Mallmann R, Oksche A.** Deen PM. Lack of arginine vasopressin-induced phosphorylation of aquaporin-2 mutant AQP2-R254L explain dominant nephrogenic diabetes insipidus. *J. Am. Soc. Nephrol* 2005; 16: 2872-2880.
6. **Echevarria M, Gonzalez E, Gutiérrez A, Whitembury G.** Water and urea diffusive permeabilities in isolated proximal tubule cells. *Am. J. Physiol.* 1994; 267: F709-F715.
7. **Echevarría M, Frindt G, Preston G, Milovanovic S, Agre P, Fischbarg J, Windhager EE.** Expression of multiple water channel activities in *Xenopus* oocytes injected with mRNA from rat kidney. *J. Gen. Physiol*, 1993; 101: 827- 841.
8. **Echevarría, M., Ilundáin, A.A., Aquaporins.** *J. Physiol. Biochem.* 1998; 54: 107-118.
9. **Finkelstein A.** Water Movement Through Lipid Bilayers, Pores and Plasma Membranes. Theory and Reality. New York, John Wiley and Sons, 1987.
10. **Finkelstein A.** "The water permeability on narrow pores". In: *Isotonic Transport in Leaky Epithelia*, H.H.Ussing, J. Fischbarg, O. Sten-Knudsen, E.H. Larsen EH, N.J. Willumsen, J. Hess-Thaysen, editors. Alfred Benzon Symposium No 34, Copenhagen: Munksgaard, 1993; pp. 487-503.
11. **Ford P, Rivarola V, Chara O, Blot-Chabaud M, Cluzeaud F, Farman N, Parisi M, Capurro C.** Volume regulation in cortical collecting duct cells: role of AQP2. *Biology of the cell.* 2005; 97: 687-697.
12. **Gutiérrez AM, González E, Echevarría M, Hernández CS, Whitembury G.** "The proximal straight tubule (PST) basolateral cell membrane water channel; Selectivity characteristics." *Journal Membrane Biol*, 1995; 143: 189-9.
13. **Macey RI, Farmer REL.** Inhibition of water and solute permeability in human red cells. *Biochimica et Biophysica Acta.* 1970; 211: 104-106.
14. **Murillo-Carretero M, Ilundáin AA, Echevarría M.** Regulation of aquaporins mRNA expression in rat kidney by water intake. *J. Am. Soc. Nephrol.* 1999; 10: 696-703.

15. **Nielsen S, Digiovanni SR, Christensen EI, Knepper MA, Harris HW.** Cellular and subcellular immunolocalization of vasopressin-regulated water channel in rat kidney. *Proc. Natl. Acad. Sci. USA* 1993; 90: 11663-11667.
16. **Parisi M, Bourguet J.** The single file hypothesis and the water channels induced by antidiuretic hormone. *J Membrane Biol.*, 1983; 71: 189-193.
17. **Preston GM, Piazza-Carrol P, Guggino WB, and Agre P.** Appearance of water channels in *Xenopus* oocytes expressing red cell CHIP28 protein. *Science* 1992; 256: 385-387.
18. **Tajkhorshid E, Nollert P, Jensen Mø, Miercke LJW, O'Connell J, Stroud RM, and Shulten K.** Control of the selectivity of aquaporin water channel family by global orientational tuning. *Science* ; 296: 525-530.
19. **Takata, K, Matsuzaki T, Tajika Y.** Aquaporins: water channel proteins of the cell membrane. *Prog Histochem Cytochem.* 2004; 39: 1-83.
20. **Tosteson DC, editor.** Membrane Transport: People and Ideas. American Physiological Society, Bethesda Maryland, 1989.
21. **Verkman, AS.** Novel roles of aquaporins revealed by phenotype analysis of knockout mice. *Rev Physiol Biochem Pharmacol.* 2005. August 10. E-pub ahead of print.
22. **Walz T, Hirai T, Murata K, Heymann BJ, Mitsuoka K, Fujiyoshi Y, Smith BL, Agre P, and Engel A.** The three-dimensional structure of aquaporin-1. *Nature* 1997; 387: 624-627.
23. **Whittembury G, Carpi-Medina P, González E, Linares H.** Effect of parachloromercury-benzene-sulfonic acid and temperature on cell water osmotic permeability of proximal straight tubules. *Biochim. Biophys. Acta* 1984; 775: 365-373.
24. **Whittembury G, Gonzalez E, Gutierrez AM, Echevarria M & Hernandez CS.** Length of the selectivity filter of Aquaporin-1. *Biology of the Cell* 1997; 89: 299-306.
25. **Whittembury G, Hill AE.** Coupled transport of water and solutes across epithelia. In *The Kidney, Physiology and Pathophysiology*, 3rd edition, (D. Seldin, G. Giebisch, editors.) New York: Lippincott Williams & Wilkins, Chapter 14, pp 341-362. 2000.
26. **Whittembury G, Lindemann B, Carpi-Medina P, González E, Linares H.** Continuous measurements of cell volume changes in single kidney tubules. *Kidney International*, 1986; 30: 187-191.
27. **Whittembury G, Reuss L.** "Mechanisms of coupling of solute and solvent transport in epithelia". In: *The Kidney: Physiology and Pathophysiology*, 2nd edition, (D. Seldin, G. Giebisch editors.) New York: Raven Press, Chapter 11, pp.: 317-60. 1992.
28. **Yasui M, Hazama A, Kwon TH, Nielsen S, Guggino WB, Agre P.** Rapid gating and anion permeability of an intracellular aquaporin. *Nature* 1999; 402: 184-187.
29. **Zeuthen T, Klaerke DA.** Transport of water and glycerol in aquaporin 3 is gated by H⁺. *J. Biol.Chem* ; 274: 21631-21636.



Argentine
Physiological
Society
